TU Delft
Bibliotheek
Prometheusplein 1
Postbus 98
2600 MG DELFT

Telefoon: 015 - 2784636
Fax: 015 - 2785673
Email: Helpdesk.doc@Library.TUDelft.NL

Datum: 04-apr-05

Bonnummer: 874988

Aan: UVA KEUR

BROERSTRAAT 4
9700 AN GRONINGEN
NEDERLAND

Tav:

Aantal kopieën: 5

Uw referentie(s): A078198844
UVA KEUR

Artikelomschrijving bij aanvraagnummer: 874988

Artikel: Long term X-ray observations of SMC X-1 including a turn-o
Auteur: J.M. Bonnet-Bidaud, M. van der Klis
Tijdschrift: ASTRONOMY AND ASTROPHYSICS
Jaar: 1981 **Vol.** 97 **Aflevering:**
Pagina(s): 134-138 **Plaatsnr.:** 8477 C

Astron. Astrophys. 97, 134–138 (1981)

ASTRONOMY AND ASTROPHYSICS

Long Term X-ray Observations of SMC X-1 Including a Turn-on

J. M. Bonnet-Bidaud[1] and M. van der Klis[2]

[1] Section d'Astrophysique, CEN-SACLAY, B.P. No. 2, F-91190 Gif-sur-Yvette, France
[2] Astronomical Institute, University of Amsterdam and Cosmic Ray Working Group, Leiden, The Netherlands

Received March 14, accepted October 13, 1980

Summary. A 38 d COS-B observation of SMC X-1 in the 2–12 keV band is presented, which includes a turn-on of this source.

The data are discussed within the frame work of the stellar wind accretion model, both from the point of view of the expected accretion rate and of the absorption of X-rays in the wind.

Neither the high state luminosity nor the on-off behaviour of this source can be satisfactorily explained by this model.

Key words: X-ray binaries – stellar wind – COS-B

I. Introduction

The X-ray source SMC X-1 was discovered by Price et al. (1971) and was subsequently identified as a binary system (Schreier et al., 1972); the optical companion is a B 0 I supergiant (Webster et al., 1972). After the discovery of the X-ray pulsator in SMC X-1 (Lucke et al., 1976), further observations have been devoted to the determination of the spin-up rate (Henry and Schreier, 1977) and the orbital elements of the system (Primini et al., 1976; Davison, 1977; Primini et al., 1977).

The X-ray source is known to be variable in both spectral shape and luminosity. In the high state the source is very bright, having a luminosity around $5\ 10^{38}$ erg s^{-1} (Clark et al., 1978). Extended low states have been reported during which the luminosity drops by more than a factor 10 (Schreier et al., 1972; Cooke et al., 1978; Tuohy and Rapley, 1975). This kind of behaviour makes SMC X-1 very comparable to another massive X-ray binary, Cen X-3 for which useful information on accretion processes was drawn from turn-on studies (Schreier et al., 1976; Bonnet-Bidaud and van der Klis, 1979).

Nevertheless, the short duration of the previous observations of SMC X-1 did not yet allow the study of a transition between a low and a high state in this source.

In this paper, we report data obtained with the X-ray detector on board the ESA COS-B satellite during a 38 d observing run which fully covered such a transition of the source.

The similarity with Cen X-3 has led us to investigate whether the stellar wind from the companion is also responsible for the on-off behaviour, as has been proposed for Cen X-3 (Schreier et al., 1976; Carlberg, 1979).

II. Observations

The detector on board the COS-B satellite is a 80 cm^2 collimated proportional counter with an energy band of 2–12 keV (see Boella et al., 1974).

The satellite was pointed to the position of SMC X-1 for 37.7 d between 1976 Nov. 2.7 and 1976 Dec. 10.4.

Other SMC sources, SMC X-2 and SMC X-3 were also in the 10° FWHM field of view, as well as 4 U 0052–68. They may have contributed up to ~ 0.4 c/s to the total counting rate if they were at their maximum intensity (Clark et al., 1978).

Figure 1 is a plot of the counting rate during this observation. Each 68 min bin represents the average of 40 equally spaced 25.4 s integrations of the 2–12 keV intensity. The curve shows gaps of ~ 10 h every 36 h which are due to the passage of the satellite through the radiation belts. Particle background variations were substracted by using correlation formulae determined from pointings to empty fields. The typical 1σ error per bin derived from counting statistics is ~ 0.6 c/s. There is no evidence of non-statistical short term background variability. As the absolute level of the background is only known to an accuracy of ~ 1 c/s, and because of the possibility that other sources than SMC X-1 contributed to the counting rate, the zero level was adapted such that the level of the first 16 d of the observation was set equal to zero, as SMC X-1 was below the detection threshold during that time (see below).

The dashed lines in Fig. 1 mark the eclipse limits computed from the ephemeris and eclipse duration derived by Davison (1977). Before JD 2443102, the counting rate during the predicted eclipses is not significantly different from that during the uneclipsed intervals. After that time the source is seen to exhibit the characteristic eclipsing binary behaviour. The intensity is still somewhat attenuated during binary cycles 5 and 6, especially near to the eclipses, but starting from cycle 7 the counting rate during non-eclipse is rather constant at 3.5–4.0 c/s, equivalent to about 40 Uhuru counts. [1 COS-B c/s $\sim 2.9\ 10^{-10}$ erg cm^{-2} s^{-1} (2–12 keV) for a Crab spectrum].

The turn-on of SMC X-1 presented here is similar to observations of this phenomenon in Cen X-3 published earlier (Schreier et al., 1976; Bonnet-Bidaud and van der Klis, 1979). The intensity transition takes place on a similar time scale: 1–2 binary cycles, i.e. 4–8 d. In cycle 5 the light curve shows a higher intensity around phase 0.5 than near to the eclipses, though there is no evidence for an intensity spike near this phase as in the Uhuru observation of a Cen X-3 turn-on.

Figure 2 shows these data folded modulo the binary period. The observations were divided into two parts, with the boundary at JD 2443101. The difference between the eclipsed and uneclipsed counting rates during the low state is 0.11 ± 0.09 c/s, so the source was at a level below 0.2 c/s during this time. The mean uneclipsed intensity during cycles 5–10 is 3.28 ± 0.04 c/s, the mean eclipse

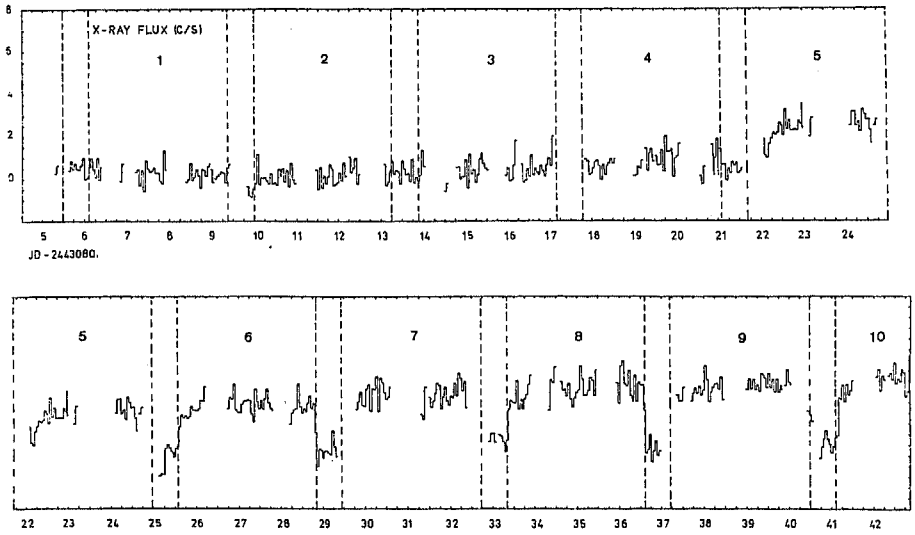

Fig. 1. The counting rate from the region of SMC X-1 during the 38 d observing period. The typical error in one 68 min bin is ~0.6 c/s. Dashed lines show predicted eclipse limits. Contaminating sources contribute less than 0.4 c/s

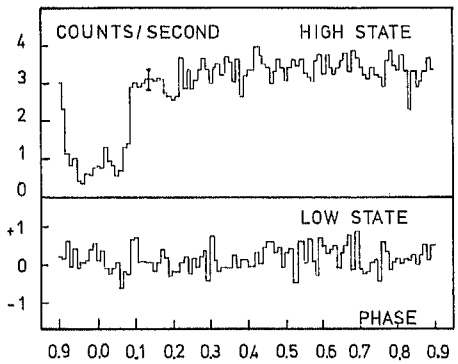

Fig. 2. The counting rate data folded modulo the binary period separately for: **a** the first part of the observation (low state), and **b** the second part (high state). Typical 1 σ error is shown. The zero level was adapted to the mean counting rate in the low state

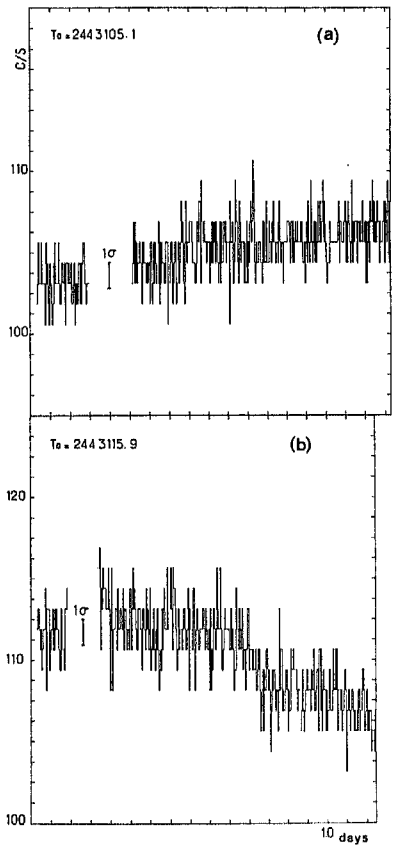

Fig. 3 a and b. Eclipse transitions. The counting rate during two eclipses transitions at ~200 s resolution. Data are uncorrected for background. Typical counting statistics error bars are shown. Note the difference between the gradual transition in **a** and the much better defined one in **b**

intensity 0.83 ± 0.07 c/s, slightly higher than the low state counting rate.

As can be seen from Fig. 1, the data cover five eclipse transitions: both the eclipse entrance and exit at the start and the end of binary cycles 6 and 8, and one more eclipse exit at the beginning of cycle 10. From full time resolution (~200 s) plots of the data, one can see that the eclipse transitions show noticeable changes from cycle to cycle. (See Fig. 3).

In binary cycle 6, the transitions are still somewhat irregular in shape and last about 0.1–0.2 d. In cycle 8, however, they are quite sharp with a duration of ~0.04 d and similar in shape. The eclipse exit in cycle 10 is slightly less well defined and takes ~0.08 d. The heliocentric mid-transition times of the latter three cycles were determined to be JD 2443113.3706 ± 0.0024, JD 2443116.6214 ± 0.0024 and JD 2443121.164 ± 0.007, respectively.

From these three times one can derive a mean eclipse duration of 0.646 ± 0.005 d ($\theta_E = 29\overset{\circ}{.}9 \pm 0\overset{\circ}{.}2$), and a mid-eclipse time (phase 0.0) ϕ_0 = JD 2443116.9443 ± 0.0022, assuming symmetry of the eclipses around ϕ_0. This eclipse duration is somewhat long compared to earlier measurements (Primini et al., 1977; Davison, 1977), so care should be taken in the interpretation of these results since absorption effects may be important near the eclipses. The present determination carries the total number of published measurements of the mid-eclipse time to six (Table 1).

Figure 4 shows the resulting mean orbital period determinations as a function of time. It should be noted, that only three of the five points in this plot are independent.

Table 1. Mid-eclipse time determinations of SMC X-1

Observation	N (period number)	(Mid-eclipse times)	Ref.
Uhuru	0	2440964.49 ± 0.02	Schreier et al. (1972)
Optical	232	2441867.44 ± 0.04	van Paradijs (1977)
Copernicus	337	2442276.15 ± 0.04	Tuohy and Rapley (1975)
SAS-3	481	2442836.6823 ± 0.0002	Primini et al. (1977)
Ariel V	523	2443000.1562 ± 0.0016	Davison (1977)
COS-B	553	2443116.9443 ± 0.0022	This paper

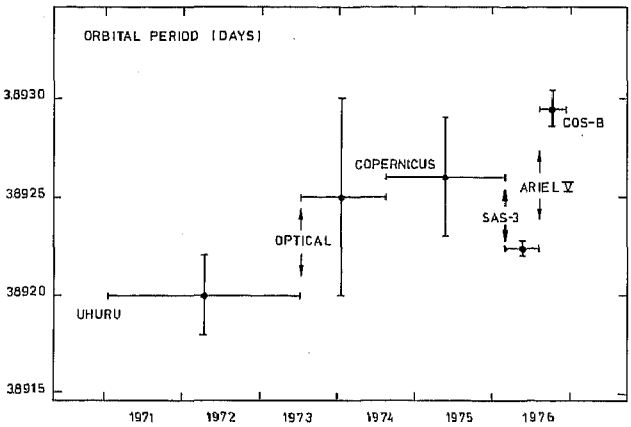

Fig. 4. The evolution of the orbital period of SMC X-1 as determined from the six independent ϕ_0 measurements given in Table 1. Horizontal bars represent the time between two ϕ_0 determinations, vertical bars are the 1 σ errors of the resulting mean P_{orb}.

A linear least-squares fit to the six points in Table 1 yields a value for the mean orbital period between Jan. 1971 and Dec. 1976 of $P_{orb}=3.89239\pm0.00007$ with $\phi_0=2449064.444\pm0.033$; fitting to a quadratic function of the form $\phi_0=t_0+P_{orb}N+\frac{1}{2}\dot{P}_{orb}P_{orb}N^2$ where N is the number of binary periods, gives a formal value of $\dot{P}_{orb}/P_{orb}$ of $+(1.2\pm1.5)\,10^{-5}$ yr^{-1}, but does not improve the fit which is quite poor in both cases. The high Xhi-square value $X^2\sim10$ both for the linear and the quadratic fit, may reflect underestimation of the errors or fluctuations of the orbital period. A longer time span of observations is clearly necessary to conclude on any general trend in the orbital period.

III. Discussion

a) Wind Accretion

From the observed maximum counting rate of ~4.0 c/s (see Fig. 1) for the last on-state cycles of the source, the 2–12 keV luminosity can be derived using the Crab source as a calibration for the detector. The source spectrum was assumed to be best represented by a power-law with photon spectral index $\alpha=1.15\pm0.15$ as indicated by recent spectral observations (Ulmer, 1975; Davison, 1977; Clark et al., 1978).

The computed luminosity is then $L_x=(5.4\pm0.3)\,10^{38}$ erg s^{-1} for a distance to the Small Magellanic Cloud of 65 kpc (Gascoigne, 1974). This luminosity is similar to the one derived for the same energy band from observations by Ariel V (Davison, 1977) and SAS-3 (Clark et al., 1978).

As noted before (Petterson, 1978; Conti, 1978), this L_x is too high to be explained by accretion from the stellar wind of the SMC X-1 companion.

Figure 5a shows the present information on the discrepancy between the wind accretion model and the observed L_x. The unbroken curves, calculated according to Bonnet-Bidaud and van der Klis (1979) show the mass loss of the primary required to account for an L_x of 5.4 10^{38} erg s^{-1}, as a function of the terminal velocity of the wind for two different wind profiles (Castor et al., 1975; hereafter called CAK, and Abbot, 1978). These two profiles can be considered as extremes that bracket the real velocity law for a radiatively driven wind (Conti, 1978). Curves are given for co-rotating (CR) and no-rotating (NR) primary, which is assumed to fill the corresponding critical lobe (Pratt and Strittmatter, 1976). The terminal velocity of the wind V_T can be estimated to be about three times the escape velocity at the surface of the primary (Lamers et al., 1976). This relation is supported by recent IUE observations of OB stars (Hutchings and van Rudlof, 1979) and of other massive binaries (Dupree et al., 1978, 1979).

For the range of values for V_T (computed from Lamers relation), allowed by the uncertainties in the stellar parameters (vertical lines, Fig. 5a), the mass loss rate required to feed the source at the observed luminosity ranges from 10^{-3} to $10^{-5}M_\odot$ yr^{-1}. This strongly exceeds the wind mass-loss rate found in early-type supergiants (Hutchings, 1976; Barlow and Cohen, 1977) and the maximum mass-loss rate by radiation-driven wind (Cassinelli and Castor, 1973) obtained when all the momentum of the emitted photons is transferred to the wind. (Dashed curve in Fig. 5a). [A luminosity of the companion of $L_*=8.8\,10^{38}$ erg s^{-1} (van Paradijs and Zuiderwijk, 1977) was assumed to calculate this curve].

The discrepancy amounts to a factor 5 for the Abbot profile and to more than two orders of magnitude for the CAK model, while commonly observed values for $\dot{M}_*$ are of the order of 50% of this theoretical limit (Barlow and Cohen, 1977). Stellar wind could only account for the observed X-ray luminosity if it were highly asymmetric, favouring the orbital plane with a higher particle density, or if the presence of the X-ray source would greatly reduce the acceleration of the wind, resulting in a surprisingly low terminal velocity: $V_T\sim1200$ km s^{-1} for the Abbot profile and $V_T\sim500$ km s^{-1} for the CAK profile.

b) Wind Absorption

Further information on the accretion mechanism in SMC X-1 can be drawn from the fact that the observed flux during most

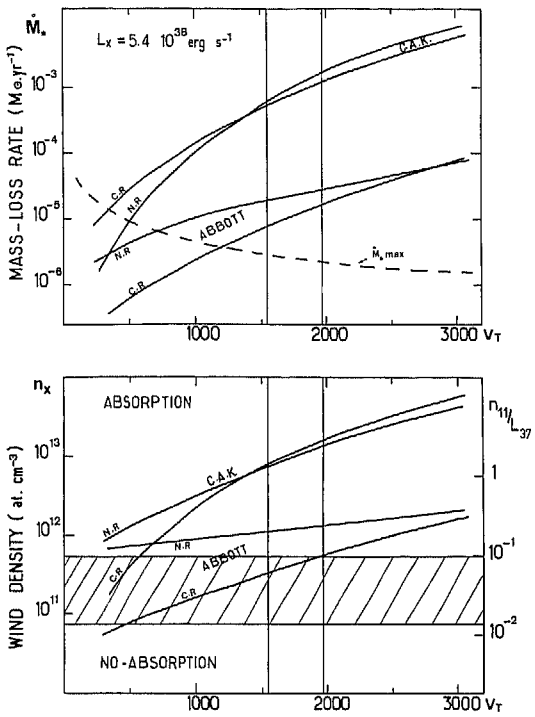

Fig. 5a and b. Stellar wind accretion. **a** The mass-loss rate of the primary star required to produce an X-ray luminosity of 5.4 10^{38} erg s^{-1} as a function of the terminal velocity of the wind. Curves are given for two different acceleration models, Abbot and CAK which can be considered as limits (see text), and for the following system parameters: $M_*=16\ M_\odot$, $M_x=1\ M_\odot$, $a=1.74\ 10^{12}$ cm ($i=67°$) (drawn curves). The primary star is assumed to reach its substellar radius computed according to Pratt and Strittmatter (1976) for two different assumptions regarding the rotation (no rotation, N. R. and corotation, C. R.). Also shown is the maximum theoretical mass-loss rate ($\dot{M}_{max}$) for radiation-driven winds (dashed curve). Vertical lines show the predicted range of values for V_T (see text). In this range, the required mass-loss exceeds the maximum value by factors ranging from 5 to 400. **b** The density of the wind near the X-ray star required to produce a X-ray luminosity of 5.4 10^{38} erg s^{-1} as a function of the terminal velocity under the same conditions as in Fig. 4a, assuming the mass loss rate really exceeds the maximum value. Hatched area represents the limiting density for the occurrence of absorption for a variety of incident X-ray spectra and assumptions for the velocity profile. The relative position of the curves is independent of L_x (right hand scale) (see text)

part of the high luminosity cycles seems to be unaffected by wind absorption. In fact, absorption in a stellar wind would cause a phase dependence of the flux as observed for Cen X-3 by Pounds et al. (1975) and Schreier et al. (1976), while the on-state cycles actually show a constant flux and rather sharp eclipse transitions. So, in spite of the fact that no spectral data are available during this observation, it is most likely that wind absorption is negligible during most of the high L_x cycles.

For a spherically symmetric wind and standard accretion efficiency, the required particle density near the X-ray star n_x is for a fixed X-ray luminosity L_x a function of the relative wind velocity V_{rel} only

$$n_x = \frac{L_x}{\eta c^2 m_H} \frac{V_{rel}^3}{4\pi (GM_x)^2}$$
$$= 2.98\ 10^{11} \left(\frac{L_x}{10^{37}\ \text{erg s}^{-1}}\right) \left(\frac{V_{rel}}{1000\ \text{km s}^{-1}}\right)^3 \text{at cm}^{-3}$$

where η is the conversion factor of rest-mass to X-rays, M_x is the mass of the X-ray star ($\sim 1\ M_\odot$) and m_H is the proton mass.

This required density is shown in Fig. 5b for SMC X-1 as a function of terminal velocity of the wind for an L_x of 5.4 10^{38} erg s^{-1} and the same assumptions on wind profile and primary rotation as in Fig. 5a. Along these curves, the mass loss rate increases to compensate the reduction of accretion efficiency for larger wind velocities. For the range of values for V_T considered in IIIa, the required density is seen to be $n_x \sim 5\ 10^{11}$ at cm^{-3} and 10^{13} at cm^{-3} for the Abbot and CAK profiles respectively, assuming corotation.

A good order of magnitude estimate of the limiting density required for absorption to occur can be derived from the model of Hatchett and Mc Cray (1977) for X-ray radiation transfer through the stellar wind. In this model, the photoionisation of oxygen ions is taken to be the main source of opacity up to 7 keV. We will adopt this process to be the dominant source of absorption, since with the present 2–12 keV detector response, 70% of the counts in the detector will be provided by the (2–7 keV) photons, even, if we assume a flat energy spectrum for the source (Lucke et al., 1976).

As shown by Hatchett and Mc Cray (1977), the structure of ionisation regions around the X-ray star can be described by a single parameter:

$$q = \xi / (L_x / n_x a^2)$$

where a is the orbital separation and ξ is a parameter which completely describes the ionisation state of an optically thin gas for a given incident spectrum. The limiting density for absorption can then be derived from the value of q for which the ionisation surface becomes closed around the X-ray star. As the spectral shape of SMC X-1 is found to be variable and cannot be determined from the present observations, we have adopted the range of values for log ξ of 2.7–3.5 given by Hatchett and Mc Cray (1977) for different spectra. A certain range in q was also taken into account to allow for the uncertainty of the velocity profile.

The resulting range in density is shown in Fig. 5b by the hatched area. It is clear that within the expected range of terminal velocities (vertical lines), the density required to produce the observed X-ray luminosity by wind would at the same time be responsible for an appreciable absorption of the flux. The resulting light curves during high state should therefore be similar in shape to the curve computed by Hatchett and Mc Cray (1977) for Cen X-3, which shows a clear phase dependent absorption. Such features are not present in the observed flux outside eclipses, as is apparent from Fig. 1.

With respect to the observed turn-on, we note that in the picture of wind accretion, both the wind density required to feed the source and the limiting density for absorption scale as L_x, so that the *relative* positions of the curves in Fig. 5b are not affected by differences in the intrinsic luminosities. A turn-on of the source as observed here, cannot therefore be caused by a change in the wind mass-loss rate alone, since at constant wind velocity the change in absorption would exactly compensate the change in intrinsic luminosity. Such a turn-on could then – in the case of

wind accretion – only be the result of a decrease of the wind velocity.

A similar result was obtained by Carlberg (1979) who computed the wind velocity near the X-ray star to decrease from 800 to 500 km s^{-1} during a turn-on of Cen X-3 while the intrinsic luminosity remains nearly constant at $\sim 5\ 10^{37}$ erg s^{-1}. It should be noted, however, that the mass-loss rate of $2\ 10^{-5}\ M_{\odot}\ yr^{-1}$ required in this model to power the X-ray source by wind accretion seems rather prohibitive for the same reasons as given in Sect. IIIa. The effect of decreasing the wind velocity to produce the turn-on will be to increase appreciably the intrinsic luminosity going from the off-state to the on-state, since L_x scales approximatively as $V_T^{-4}\dot{M}_*$. This prediction of the stellar wind accretion model is not in accordance with an observation of a turn-on in Cen X-3 (van der Klis et al., 1979), where the intrinsic luminosity was inferred from the spin-up rate of the neutron star to be higher during the low state than after the turn-on.

Conclusion

The long duration of the present observation of SMC X-1 made it possible to study a turn-on of the source and the subsequent high state over more than 20 d. Mass transfer from the primary to the neutron star by stellar wind alone is found to be unable to account for the observed high state luminosity, the absence of a phase-dependant absorption in the high state and the on-off behaviour of the source. However, if the accreted matter is fed to the neutron star in another way (i.e., by Roche lobe overflow), absorption by a surrounding stellar wind could be responsible for the on-off behaviour as pointed out for Cen X-3 by Schreier et al. (1976). In this case, the intrinsic luminosity during the low state is expected to be lower than during the high state, which means that a useful check could come from study of the spin-up rate during the turn-on. At least in Cen X-3, such a study indicates on the contrary a higher L_x during the low state (van der Klis et al., 1979).

A more hopeful picture may be one in which the accretion as well as the bulk of the absorption of the X-rays are due to matter provided by Roche-lobe overflow. The stellar wind would then be responsible only for a small part of the accreted matter and for some secondary phase-dependant absorption. In this case, the similar on-off behaviour found in both the sources SMC X-1 and Cen X-3 could be due to quasi-periodic changes in mass-loss rate, for example originating from *g*-mode waves at the surface of the primary star modulating the Roche lobe overflow (Papalaizou, 1979; Savonije, 1979).

Acknowledgements. It is a pleasure to thank E. P. J. van den Heuvel and H. F. Henrichs for reading of the manuscript and useful discussion.

M. van der Klis acknowledges support by the Netherlands Organisation for Pure Research (ZWO).

References

Abbot, D.: 1978, *Astrophys. J.* **225**, 893
Abbot, D.: 1977, Ph.D.Thesis, Univ. of Colorado
Barlow, M., Cohen, M.: 1977, *Astrophys. J.* **213**, 737
Boella, G., Buccheri, R., Burger, J.J., Coffaro, P., Paul, J.: 1974, Proc. 9th ESLAB Symp. ESRO SP-106, 345
Bonnet-Bidaud, J.M., van der Klis, M.: 1979, *Astron. Astrophys.* **73**, 90
Bradt, H., Doxsey, R., Jernigan, J.: 1978, IAU COSPAR *Symp.* Innsbruck
Carlberg, R.: 1979, *Astrophys. J.* **232**, 878
Cassinelli, J., Castor, J.: 1973, *Astrophys. J.* **179**, 189
Castor, J., Abbot, D., Klein, R.: 1975, *Astrophys. J.* **195**, 15
Clark, G., Doxsey, R., Li, F., Jernigan, J.G., van Paradijs, J.: 1978, *Astrophys. J.* **221**, L37
Conti, P.: 1978, *Astron. Astrophys.* **63**, 225
Cooke, B.A. et al.: 1978, *Monthly Notices Roy. Astron. Soc.* **182**, 489
Davidson, K., Ostriker, J.P.: 1975, *Astrophys. J.* **179**, 585
Davison, P.J.N.: 1977, *Monthly Notices Roy. Astron. Soc.* **179**, 15P
Dupree, A. et al.: 1978, *Nature* **275**, 400
Dupree, A., Gursky, H., Black, J., Davis, R., Hartmann, L., Matilsky, T., Raymond, J., Hammerschlag-Hensberge, G., van den Heuvel, E., Lamers, H., van den Bout, P., Morton, D., de Loore, C., Burger, M., van Dessel, E., Menzies, J., Whitelock, P., Watson, M., Sanford, P.: 1979, *Astrophys. J.* **238**, 969
Gascoigne, S.: 1974, *Monthly Notices Roy. Astron. Soc.* **166**, 25P
Hatchett, S., Mc Cray, R.: 1977, *Astrophys. J.* **211**, 552
Henry, P., Schreier, P.: 1977, *Astrophys. J. Letters* **212**, L13
Hutchings, J.B.: 1976, *Astrophys. J.* **203**, 438
Hutchings, J., Crampton, D., Osmer, P.: 1977, *Astrophys. J.* **217**, 186
Hutchings, J., von Rudlof, I.: 1979 (preprint)
Klis, M. van der, Bonnet-Bidaud, J.M., Robba, N.: 1980, *Astron. Astrophys.* **88**, 8
Lamers, H., van den Heuvel, E., Petterson, J.: 1976, *Astron. Astrophys.* **49**, 327
Lucke, R., Yentis, D., Friedmann, H., Fritz, G., Shumann, S.: 1976, *Astrophys. J. Letters* **206**, L25
Papalaizou, J.: 1979, *Monthly Notices Roy. Astron. Soc.* **186**, 791
Paradijs, J. van: 1977, *Astron. Astrophys. Suppl.* **29**, 339
Paradijs, J. van, Zuiderwijk, E.: 1977, *Astron. Astrophys.* **61**, L19
Petterson, J.: 1978, *Astrophys. J.* **224**, 625
Pounds, K., Cooke, B., Richetts, M., Turner, M., Elvis, M.: 1975, *Monthly Notices Roy. Astron. Soc.* **172**, 473
Pratt, J., Strittmatter, P.: 1976, *Astrophys. J. Letters* **204**, L29
Price, R., Groves, D., Rodriques, R., Seward, F., Swift, C., Toor, A.: 1971, *Astrophys. J. Letters* **168**, L7
Primini, F., Rappaport, S., Joss, P.C., Clark, G.W., Lewin, W., Li, F., Mayer, W., McClintock, J.: 1976, *Astrophys. J.* **210**, L71
Primini, F., Rappaport, S., Joss, P.: 1977, *Astrophys. J.* **217**, 543
Savonije, G.J.: 1979, talk presented at Advanced Study Institute on Galactic X-ray sources, Cape Sounion, Greece
Schreier, E., Giacconi, R., Gursky, H., Kellog, E., Tananbaum, H.: 1972, *Astrophys. J.* **178**, L71
Schreier, E., Swartz, K., Giacconi, R., Fabbiano, G., Morin, J.: 1976, *Astrophys. J.* **204**, 539
Tuohy, I.R., Rapley, C.G.: 1975, *Astrophys. J.* **198**, L69
Ulmer, M.P.: 1975, *Astrophys. J.* **196**, 827
Webster, B., Martin, W., Feast, M., Andrews, P.: 1972, *Nature Phys. Sci.* **240**, 183